Reverse engineering of multilayer coatings for ultrafast laser applications

M. Trubetskov,[1,2,*] T. Amotchkina,[2] A. Tikhonravov,[2] and V. Pervak[3,4]

[1]Max-Planck Institute of Quantum Optics, Hans-Kopfermann-Str. 1, 85748 Garching, Germany

[2]Research Computing Center, Moscow State University, Leninskie Gory, 119991 Moscow, Russia

[3]Ludwig-Maximilians-Universitaet Muenchen, Am Coulombwall 1, 85748 Garching, Germany

[4]Ultrafast Innovations GmbH Am Coulombwall 1, 85748 Garching, Germany

*Corresponding author: Michael.Trubetskov@mpq.mpg.de

Received 29 August 2013; accepted 21 October 2013;
posted 29 October 2013 (Doc. ID 196689); published 3 December 2013

We propose a reliable reverse engineering approach for a postproduction characterization of complicated optical coatings for ultrafast laser applications. We perform the postproduction characterization on the basis of *in situ* broadband monitoring data and validate the results using *ex situ* transmittance data and group delay measurements. © 2013 Optical Society of America

OCIS codes: (310.3840) Materials and process characterization; (310.6860) Thin films, optical properties; (310.6805) Theory and design; (320.7080) Ultrafast devices; (320.5520) Pulse compression.
http://dx.doi.org/10.1364/AO.53.00A114

1. Introduction

Determination of actual parameters of layers of produced multilayer samples [reverse engineering (RE) of optical coatings] provides feedback to the modern design-production chains and allows optical coating engineers to improve the deposition process. This includes adjustment of deposition parameters, recalibration of the monitoring system, correction of tooling factors, etc. [1–4]. The reliability of the RE results depends on the experimental data set as well as on the stability of the corresponding numerical algorithms [1,3,5]. Some numerical algorithms (for example, sequential algorithm processing transmittance scans recorded *in situ* during the deposition) cannot provide correct RE results [5,6]. Insufficient information content of input experimental data may lead to unstable meaningless RE solutions (for example, *ex situ* transmittance and/or reflectance measurements that do not contain informative features in the spectral range of measurements) [1].

One approach to increase RE reliability is to involve more experimental information in the RE process, for example, to use transmittance/reflectance scans recorded *in situ* in the course of the deposition process [1,5,6], to perform *ex situ* measurements in a wider spectral region [1], to explore combinations of different types of data (for example, spectrophotometric and ellipsometric data) [7], and to take multiangle measurements into consideration [8,9].

A second approach to improve the stability of the RE results is to use all available *a priori* information regarding the considered coatings and deposition process. This may include estimations of the level of errors in layer thicknesses derived by careful characterization or information regarding the stability/instability of refractive indices of thin-film materials [2,3], the presence/absence of bulk inhomogeneity, surface roughness, etc.

A third approach to raise the reliability of the RE results is to verify these results using the experimental data that were not involved in the RE algorithm.

1559-128X/14/04A114-07$15.00/0

For validation of RE results, various methods may be applied. In Ref. [5], special coatings with imposed errors on layer thicknesses were produced. The numerical algorithm used for RE of these coatings reproduced the errors with high accuracy. Spectrophotometric data measured at a set of incidence angles may be useful for verification of RE solutions [4]. In practical RE problems, all three approaches listed above and their combinations should be used.

In this paper we consider RE problems related to complicated multilayer coatings for ultrafast laser applications. These coatings form a special class of multilayers because along with the conventional reflectance/transmittance, target group delay (GD) or group delay dispersion (GDD) is specified. Ultrafast laser applications often require broadband coatings with a working spectral range of about one optical octave. The specific feature of these coatings is that they typically contain many (more than 50) layers and spectral characteristics (especially GD and GDD) are very sensitive to unavoidable deposition errors in layer thicknesses and deviations of layer material refractive indices. Typically, in order to design such multilayers, special design techniques and approaches are required [10–16]. A large number of coating layers may easily cause instability in the course of RE of these coatings. In this paper we propose a reliable RE approach for such complicated coatings. In our approach we include three sets of measurement data, namely, transmittance spectra recorded *in situ* after deposition of each layer, transmittance data taken *ex situ* in a broadband spectral range, and GD/GDD experimental data. Our RE algorithm exploits *a priori* information about the level of thickness errors. Finally, the main feature of our approach is a verification of the RE results with the help of GD/GDD measurements. In our approach, therefore, we use a combination of all three tools mentioned above.

In order to demonstrate our RE approach, we considered multilayer coatings for three different types of ultrafast laser applications. In Section 2 we briefly describe the considered design problems, the experimental samples produced on the basis of these designs, and the corresponding measurement data. In Section 3 we compare two RE approaches and select the reliable one. The data in Section 3 are related to the coatings of the first type. In Section 4 we apply our approach to RE of samples of two other types. In Appendix A we present results on the uniformity estimation of the produced samples. The final conclusions are presented in Section 5.

2. Experimental Samples and Measurement Data

In order to demonstrate our RE approach, we considered three problems of designing optical coatings for laser applications, produced samples of the designed coatings, obtained experimental data, and performed RE of the samples. For design purposes, OptiLayer software was used [17], and RE was performed with the help of the OptiRE module of OptiLayer software.

In all three problems, we used Nb_2O_5 as a high index material and SiO_2 as a low index material. The substrates were Suprasil of 6.35 mm thickness and B260 Glass of 1 mm thickness. The refractive index wavelength dependencies of thin-film materials and substrates are described by a well-known Cauchy formula:

$$n(\lambda) = A_0 + A_1(\lambda_0/\lambda)^2 + A_2(\lambda_0/\lambda)^4, \qquad (1)$$

where A_0, A_1, A_2 are dimensionless parameters, $\lambda_0 = 1000$ nm, and λ is specified in nanometers. The values of Cauchy parameters of thin-film materials and substrates are presented in Table 1. For brevity we use the term "theoretical" for spectral characteristics related to designed coating, and the term "model" for spectral characteristics related to coating models obtained in the course of a RE procedure.

The first problem is the design of a broadband precompensation mirror (PCM) for an optical parametric chirped pulse amplification system [18]. In this case design is performed with the double-angle approach [12] and six bounces are required in order to reach target specifications. The target reflectance is 100% in the spectral range from 700 to 1400 nm [red crosses in Fig. 1(a)]; the target GD is presented in Fig. 1(a) by blue crosses. Target GD values are divided by 6 in order to reduce GD requirements to a single mirror reflection. As a result a 74-layers design was obtained with working angles of incidence of 5° and 18° (p polarization). The black line in Fig. 1(a) corresponds to the theoretical GD calculated as a half-sum of GDs for aforementioned angles, and the green line corresponds to the theoretical reflectance for the double-angle case calculated as a geometrical mean of reflectances for two incident angles: $R_\Sigma = (R(5°)R(18°))^{1/2}$. The total physical

Table 1. Cauchy Parameters of Thin-Film Materials and Substrates

Material	A_0	A_1	A_2
Nb_2O_5	2.218485	0.021827	3.99968×10^{-3}
SiO_2	1.460472	0	4.9867×10^{-4}
Glass B260	1.502671	5.3319×10^{-3}	4.9185×10^{-4}
Suprasil	1.443268	4.06×10^{-3}	6.9481764×10^{-6}

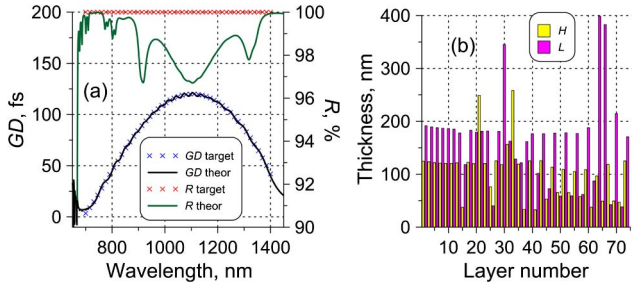

Fig. 1. (a) GD and reflectance of a 74-layers design for six-bounces double-angle PCM. (b) Physical layer thicknesses of the 74-layers PCM design.

thickness of the design is 9929 nm. Layer thicknesses are shown in Fig. 1(b).

The second problem is the design of a pulse compressor (PC) mirror. In this case it is necessary to compensate the GDD varying from -2500 fs^2 at 650 nm to -250 fs^2 at 1400 nm. In this case the double-angle approach was used again [12]; target requirements are achieved with 20 bounces using 5° and 18° angles of incidence (p polarization). As a result a 96-layers design is obtained. The total physical thickness of the PC design is 11315 nm. The target reflectance is 100% in the spectral range from 650 to 1400 nm [Fig. 2(a), red crosses]; the target GD is obtained from initial GDD specifications by integration over frequency and reduction to one bounce [Fig. 2(a), blue crosses]. The black line in Fig. 2(a) corresponds to the theoretical GD, and the green line corresponds to the theoretical reflectance; these values are calculated for the double-angle case similarly to the first design problem. Layer thicknesses are shown in Fig. 2(b).

The third problem is the design of an output coupler (OC) that is a partially reflective mirror used to extract a portion of the laser beam from the optical resonator. The target reflectance is 60%, and the target GDD is -45 fs^2 in the spectral range from 650 to 1250 nm. The obtained design solution has 68 layers; the total physical thickness is 7842 nm. The target GDD (blue crosses), target reflectance (red crosses), obtained theoretical GDD (black line), and theoretical reflectance (green line) are shown in Fig. 3(a). Layer thicknesses are shown in Fig. 3(b).

We produced designed coatings using Leybold Optics magnetron sputtering Helios plant; layer thicknesses were controlled with the help of well-calibrated time monitoring [19]. This plant is equipped with two proprietary TwinMags magnetrons and a plasma source for plasma/ion-assisted reactive middle frequency dual magnetron sputtering.

The Helios plant is also equipped with a broadband monitoring (BBM) system [20]. This system was used in a passive mode for data acquisition. We performed three deposition runs. In each run two samples were deposited simultaneously: the first of the samples was deposited on the B260 Glass substrate and the second one on the Suprasil substrate. In the first run, samples of PCM design, namely

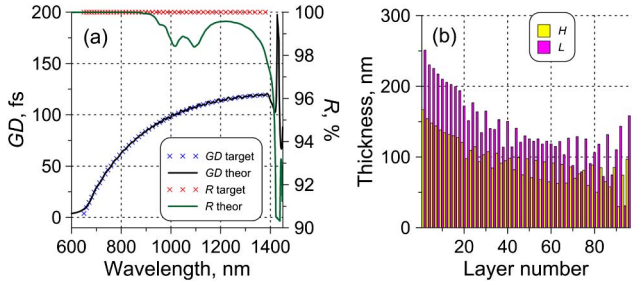

Fig. 2. (a) GD and reflectance of a 96-layers design for 20-bounces double-angle PC. (b) Physical layer thicknesses of the 96-layers PC.

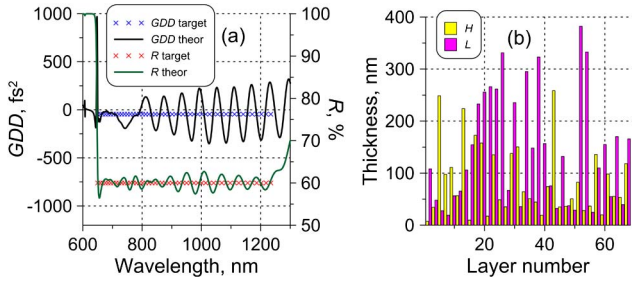

Fig. 3. (a) GDD and reflectance of a 68-layers OC design. (b) Physical layer thicknesses of the 68-layers OC.

PCM-Glass and PCM-Suprasil, were produced. In the second run, samples of PC design, PC-Glass and PC-Suprasil, were produced. In the third run, two OC samples, OC-Glass and OC-Suprasil, were produced.

The Helios plant turntable has 16 positions located at the same distance from the center of rotation. We placed all samples exactly in the middle of two sample positions of the turntable. The PCM-Glass, PC-Glass, and OC-Glass samples were placed on the position where the BBM system performed measurements. Uniformity between different positions is better than 0.2% of layer thickness and does not affect the results (see Appendix A).

For our RE process we obtained the following measurement data sets. Transmittance scans $\hat{T}^{(j)}(\lambda)$ were taken *in situ* for a set of wavelengths $\{\lambda_j\}, j = 1, \ldots, L$ after deposition of the ith layer. This data was measured using a BBM device in the wavelength range from 420 to 950 nm with the number of spectral points $L = 1195$. The BBM measurements were related to PCM-Glass, PC-Glass, and OC-Glass samples.

Transmittance data of all deposited samples were measured *ex situ* using Perkin Elmer 950 in the spectral range from 400 to 1500 nm with 1 nm wavelength step.

GD and GDD of the samples PCM-Suprasil and OC-Suprasil were extracted from the measurements provided by a white light interferometer (WLI) and processed with specially elaborated algorithm [21]. GD and GDD of the sample PC-Suprasil were measured using the recently developed resonance scanning interferometry (RSI) approach [22]. The RSI approach allowed us to obtain better accuracy of GDD since in this ultrawideband case it was possible to process all measurement data sets simultaneously [22] and to avoid the "stitching" procedure that is unavoidable in the case of WLI data processing.

3. Selection of Reliable Reverse Engineering Approach

According to our previous results [1,5], we performed RE on the basis of *in situ* transmittance measurements. We processed all transmittance scans simultaneously and used a triangular algorithm for layer parameters determination [5]. Choosing the RE

Table 2. Comparison of Discrepancy Function Values Calculated for PCM Coating

Discrepancy, %	Initial Value	Model with Random Errors	Model with Quasi-Random Errors
DF calculated on the basis of BBM data, Eq. (2)	5.5	1.90	2.0
DF calculated on the basis of *ex situ* transmittance, Eq. (5)	3.9	2.6	2.8
DF calculated on the basis of GD measurements, Eq. (4)	373.8	518.9	327.7

algorithm, we took into account the fact that the refractive indices of Nb_2O_5 and SiO_2 thin-film materials deposited in Helios plant are stable and known with high accuracy [15,19,23]. This means that refractive index variations are negligible, and deviations between theoretical and experimental data related to deposited samples can be attributed only to errors in layer thicknesses. The RE algorithm estimating errors in layer thicknesses should be carefully chosen because due to rather large numbers of layers (PCM design, $m = 74$; PC design, $m = 96$; OC design, $m = 68$), the instability of RE solutions may readily take place. We started RE of the samples with application of the algorithm assuming random errors in layer thicknesses [17]. This algorithm is based on the minimization of the *in situ* discrepancy function:

$$\mathrm{MDF}^2 = \frac{1}{mL}\sum_{i=1}^{m}\sum_{j=1}^{L}[T(X_i,\lambda_j) - \hat{T}^{(i)}(\lambda_j)]^2. \qquad (2)$$

Here $T(X_i,\lambda_j)$ is the model transmittance for the first i deposited layers assuming that there could be relative random errors $\delta_1,\ldots,\delta_m$ and relative systematic errors $\Delta_{\{H\,\mathrm{or}\,L\}}$ in layer thicknesses:

$$T(X_i,\lambda_j) = T(d_1(1+\delta_1+\Delta_H),\ldots,d_i \times (1+\delta_i+\Delta_{\{H\,\mathrm{or}\,L\}});n_H(\lambda),n_L(\lambda);\lambda). \qquad (3)$$

The initial MDF values are calculated using Eqs. (2) and (3) with $\delta_i = 0$ and $\Delta_{H,L} = 0$. In the case of the PCM-Glass sample, this value is equal to 5.5 (see Table 2). After application of the random errors model, good fitting of BBM data by model data is achieved and the MDF is decreased to a value of 1.9. Relative errors in layer thicknesses are shown in Fig. 4(a). It is seen in Fig. 4(a) that the obtained errors are quite large; some of them reach more than 10% levels. Such large values cause concerns about the reliability of the obtained RE results because it is known that the deposition process in the Helios plant is very stable and error levels in layer thicknesses do not exceed 1%–2% [15,23].

Verification of the obtained RE results was done using GD measurements. In Fig. 5(a) we compare theoretical, model, and measured GD values. Note that contrary to Fig. 1(a), here we consider single near-normal reflection; therefore GD in this case is significantly different and exhibits noticeable oscillations. Figure 5(a) shows that fitting of the experimental GD by model GD is worse than the initial correspondence between experimental and

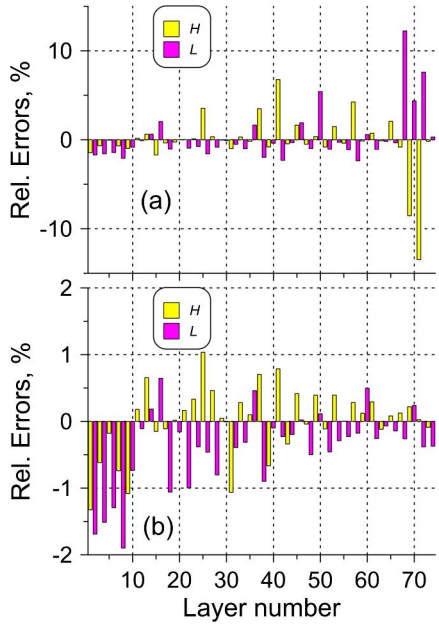

Fig. 4. Relative errors in layer thicknesses in PCM coating estimated in the frame of (a) random errors model and (b) quasi-random errors model.

theoretical GD. In order to verify RE results quantitatively, we introduce discrepancy functions $\mathrm{DF}_{\mathrm{GD}}$ and DF_T, which estimate the closeness between experimental and model data:

$$\mathrm{DF}_{\mathrm{GD}}^2 = \frac{1}{L}\sum_{j=1}^{L}[\mathrm{GD}(X,\lambda_j) - \widehat{\mathrm{GD}}(\lambda_j)]^2, \qquad (4)$$

$$\mathrm{DF}_T^2 = \frac{1}{L}\sum_{j=1}^{L}[T(X,\lambda_j) - \hat{T}(\lambda_j)]^2. \qquad (5)$$

In Eqs. (4) and (5) X is the vector of model parameters, $\widehat{\mathrm{GD}}$ is the measured GD, and $\hat{T}$ is the measured

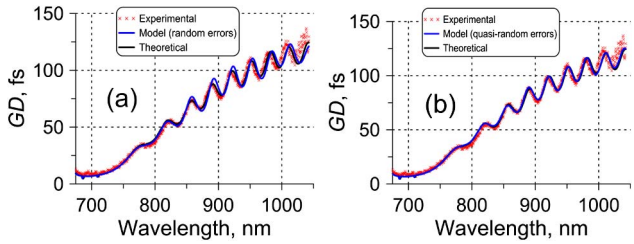

Fig. 5. Comparison of theoretical, experimental, and model GD in the case of (a) random errors model and (b) quasi-random errors model. The data are related to the PCM-Suprasil sample.

ex situ transmittance data related to the PCM-Suprasil sample. The initial DF_{GD} value calculated in the case when X defines the theoretical design is equal to 373.8. After application of the random errors model, the DF_{GD} value increased to 518.9. This increase indicates the unreliability of the RE results obtained in the frame of the random errors model. The DF_T values decreased after the application of the random errors model.

In order to prevent such unreliable RE solutions, *a priori* information related to errors in layers thicknesses must be taken into account and an appropriate model of possible errors should be chosen. In our case this *a priori* information is that the error level does not exceed 1%–2%. The corrected RE approach is based on the regularization theory of solving ill-posed problems [24]. It can be formulated as a problem of the Tikhonov's functional minimization that consists of an *in situ* discrepancy function with an additional stabilizing term:

$$\mathrm{TDF}^2 = \frac{1}{mL}\sum_{i=1}^{m}\sum_{j=1}^{L}[T(X_i,\lambda_j) - \hat{T}^{(i)}(\lambda_j)]^2 + \frac{\alpha}{m}\sum_{i=1}^{m}\delta_i^2. \tag{6}$$

In Eq. (6) α is a so-called regularization parameter that is selected to provide a compromise between data fitting and stability of the solution. The second term in Eq. (6) accounts for the stability of the solution using *a priori* information that relative random errors cannot be too big. In what follows we shall refer to this algorithm as the algorithm with quasi-random errors. We selected the regularization parameter $\alpha = 1$. The MDF value [Eq. (2)] achieved in the course of application of the algorithm with quasi-random errors is 2.0, which is almost the same value as in the case of the random errors algorithm (see Table 2). The relative errors determined by the quasi-random errors algorithm are presented in Fig. 4(b). As expected, the errors are significantly lower than in Fig. 4(a) and indeed do not exceed 2%.

In Fig. 5(b) we compare theoretical, measured, and model GD values calculated in the frame of the quasi-random model. In this figure one can observe fitting of experimental GD by model GD, which is better than initial fitting and also better than fitting achieved in the case of random errors. The achieved DF_{GD} value is 327.7 (see Table 2), which is lower than the initial DF_{GD} value (373.8) and DF_{GD} value obtained in the frame of the random errors model (518.9). The above results and considerations show that the second RE approach based on the quasi-random error model is more reliable.

4. Reverse Engineering of Pulse Compressor and Output Coupler

We apply the RE algorithm with quasi-random errors for postproduction characterization of PC samples. In Fig. 6 we show fittings of *in situ* BBM data by model data achieved in the course of the RE process. The experimental data are related to the PC-Glass sample. In Fig. 7(a) we compare theoretical, model, and experimental transmittance data related to the PC-Suprasil sample. In this figure one can observe a good fitting of experimental data by model data in the spectral range from 400 to 950 nm. At the same time, fitting in the longer wavelength range from 950 to 1500 nm is a little bit worse. The explanation for this fact is that refractive indices in the infrared spectral range are known with a lower degree of accuracy than in the visible range. In Fig. 7(b) we compare theoretical, model, and measured GDD related to the PC-Suprasil sample. It is seen that model data are in a better correspondence with the experimental data than the theoretical data. This indicates the reliability of our RE results. Relative errors estimated by the RE algorithm using the quasi-random model are shown in Fig. 8.

Finally, we apply the algorithm with quasi-random errors for RE of OC samples. In Fig. 9(a) we compare theoretical, experimental, and model transmittance

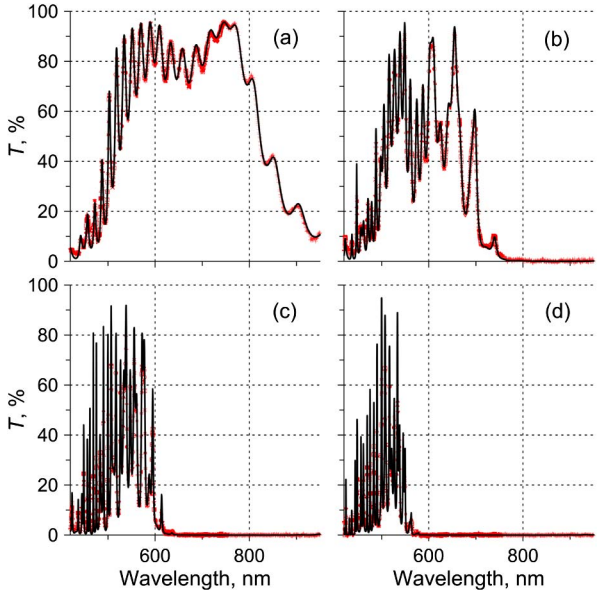

Fig. 6. Achieved fittings of BBM data by model transmittance data related to PC-Glass sample after (a) 25th layer, (b) 50th layer, (c) 75th layer, and (d) 95th layer.

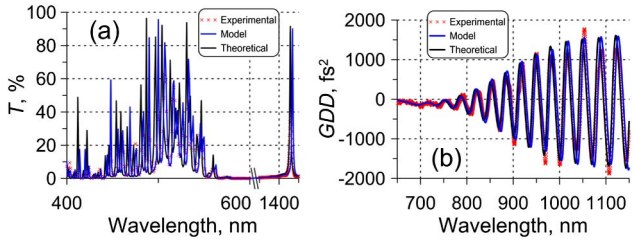

Fig. 7. Comparison of theoretical, experimental, and model transmittance (a) and GDD (b). The data are related to the PC-Suprasil sample. Transmittance is shown only in informative wavelength ranges; the high-reflection zone is omitted.

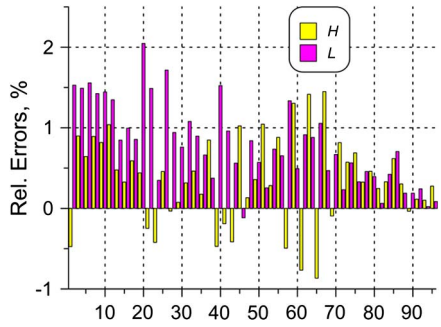

Fig. 8. Determined relative errors in layer thicknesses of PC-Glass sample.

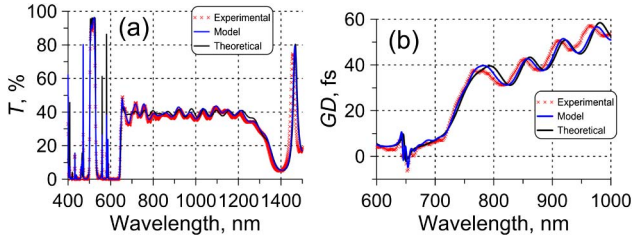

Fig. 9. Comparison of theoretical, experimental, and model transmittance (a) and GD (b). The data are related to the OC-Suprasil sample.

data related to the OC-Suprasil sample. It is seen in this figure that after application of the quasi-random model, fitting of the experimental data by model data has been significantly improved. As in the case of PC samples, fitting in the range from 400 to 950 nm is better than in the near-infrared spectral range from 950 to 1500 nm. In Fig. 9(b) we compare the theoretical, model, and measured GD related to the OC-Suprasil sample. It is seen that the model data are in a better correspondence with the experimental data than the theoretical data. This again indicates the reliability of our RE results. In Fig. 10 we show relative errors estimated by the RE algorithm. The presence of small systematic errors (about 1%) is clearly seen in Fig. 10, and this information can be used for improving the deposition quality on the next runs.

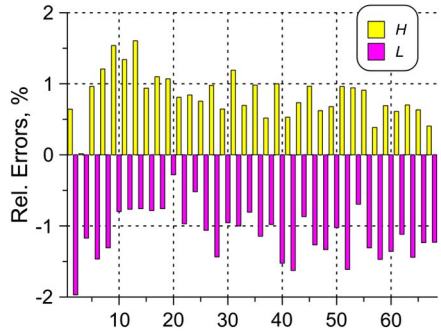

Fig. 10. Determined relative errors in layer thicknesses of OC-Glass sample.

5. Conclusions

We propose a reliable RE approach for complicated multilayers for ultrafast laser applications. In the frame of this approach, the deposited samples are characterized on the basis of *in situ* BBM data. The RE solutions are validated by comparison of the model and measured GD or GDD. The application of the proposed approach applied to the postproduction characterization of coatings of three types: PCM, PC mirror, and OC.

Appendix A: Estimation of Thickness Uniformity

In order to estimate the thickness uniformity between samples on glass and Suprasil substrates, we used transmittance data related to 21 PC samples deposited in one deposition run. 20 samples of them were deposited on Suprasil substrates, and one of them on B260 Glass substrate was placed on the test position where BBM performs measurements.

It is well known that deviation in coating thickness reveals itself in shifts of spectral curves with respect to wavelength. The ratio of corresponding wavelengths can be approximately estimated as

$$\frac{\lambda_0 + \Delta\lambda}{\lambda_0} \approx 1 + \Delta \frac{n_H + n_L}{n_H d_H + n_L d_L}, \tag{A1}$$

where λ_0 is a wavelength position, $\Delta\lambda$ is the wavelength shift, d_H, d_L are the total physical thicknesses of high and low index layers, respectively, n_H and n_L are high and low indices, respectively, and Δ is the overall physical thickness deviation for all layers. Then,

$$\frac{\Delta}{d_H + d_L} \approx \frac{\Delta\lambda}{\lambda_0} \frac{n_H d_H + n_L d_L}{(n_H + n_L)(d_H + d_L)}. \tag{A2}$$

If $\lambda_0 = 1460$ is, for example, a position of the transmittance peak between 1400 and 1500 nm of the PC sample on glass, then finding positions of this peak in transmittance data related to all 20 PC samples on Suprasil (see Fig. 11) and substituting maximum deviation $\Delta\lambda$ into Eq. (A2), we obtain an estimation of the maximum relative thickness deviation from the sample PC on glass:

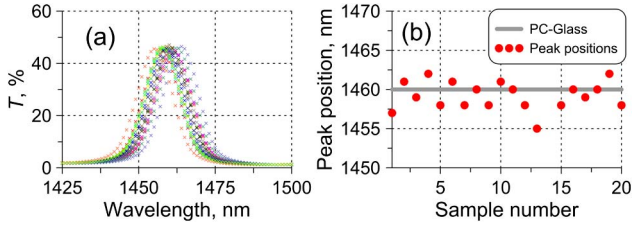

Fig. 11. (a) Experimental transmittance data related to 21 PC samples. Different colors correspond to different samples. (b) Deviations of the positions of transmittance peaks from 1460 nm.

$$\frac{\Delta}{d_H + d_L} \cdot 100\% \approx \frac{5}{1460} \frac{2.23 \cdot 4555 + 1.47 \cdot 6759}{(2.23 + 1.47)(4555 + 6759)} \cdot 100\% = 0.16\% < 0.2\%. \quad \text{(A3)}$$

In Eq. (A2) we took refractive indices of the materials equal to 2.23 and 1.47, which are refractive index values at 1460 nm (see Table 1). The deviations between transmittance peaks corresponding to different PC samples on Suprasil do not exceed 9 nm and, therefore, according to Eq. (A3), thickness deviations between different positions on the calotte do not exceed 0.3%.

This work was supported by the DFG Cluster of Excellence, "Munich Centre for Advanced Photonics" (http://www.munich-photonics.de).

References

1. T. V. Amotchkina, M. K. Trubetskov, V. Pervak, B. Romanov, and A. V. Tikhonravov, "On the reliability of reverse engineering results," Appl. Opt. **51**, 5543–5551 (2012).
2. T. V. Amotchkina, S. Schlichting, H. Ehlers, M. K. Trubetskov, A. V. Tikhonravov, and D. Ristau, "Computational manufacturing as a key element in the design–production chain for modern multilayer coatings," Appl. Opt. **51**, 7604–7615 (2012).
3. O. Stenzel, S. Wilbrandt, D. Fasold, and N. Kaiser, "A hybrid *in situ* monitoring strategy for optical coating deposition: application to the preparation of chirped dielectric mirrors," J. Opt. A **10**, 085305 (2008).
4. T. V. Amotchkina, M. K. Trubetskov, A. V. Tikhonravov, S. Schlichting, H. Ehlers, D. Ristau, D. Death, R. J. Francis, and V. Pervak, "Quality control of oblique incidence optical coatings based on normal incidence measurement data," Opt. Express **21**, 21508–21522 (2013).
5. T. V. Amotchkina, M. K. Trubetskov, V. Pervak, S. Schlichting, H. Ehlers, D. Ristau, and A. V. Tikhonravov, "Comparison of algorithms used for optical characterization of multilayer optical coatings," Appl. Opt. **50**, 3389–3395 (2011).
6. S. Wilbrandt, O. Stenzel, and N. Kaiser, "All-optical in-situ analysis of PIAD deposition processes," Proc. SPIE **7101**, 71010D (2008).
7. V. Janicki, J. Sancho-Parramon, O. Stenzel, M. Lappschies, B. Görtz, C. Rickers, C. Polenzky, and U. Richter, "Optical characterization of hybrid antireflective coatings using spectrophotometric and ellipsometric measurements," Appl. Opt. **46**, 6084–6091 (2007).
8. A. V. Tikhonravov, T. V. Amotchkina, M. K. Trubetskov, R. J. Francis, V. Janicki, J. Sancho-Parramon, H. Zorc, and V. Pervak, "Optical characterization and reverse engineering based on multiangle spectroscopy," Appl. Opt. **51**, 245–254 (2012).
9. L. Gao, F. Lemarchand, and M. Lequime, "Exploitation of multiple incidences spectrometric measurements for thin film reverse engineering," Opt. Express **20**, 15734–15751 (2012).
10. M. Trubetskov, A. Tikhonravov, and V. Pervak, "Time-domain approach for designing dispersive mirrors based on the needle optimization technique Theory," Opt. Express **16**, 20637–20647 (2008).
11. O. Nohadani, J. R. Birge, F. X. Kärtner, and D. J. Bertsimas, "Robust chirped mirrors," Appl. Opt. **47**, 2630–2636 (2008).
12. V. Pervak, I. Ahmad, M. K. Trubetskov, A. V. Tikhonravov, and F. Krausz, "Double-angle multilayer mirrors with smooth dispersion characteristics," Opt. Express **17**, 7943–7951 (2009).
13. M. K. Trubetskov, "Design of dispersive mirrors for ultrafast applications," Chin. Opt. Lett. **8**, 12–17 (2010).
14. M. K. Trubetskov, V. Pervak, and A. V. Tikhonravov, "Phase optimization of dispersive mirrors based on floating constants," Opt. Express **18**, 27613–27618 (2010).
15. V. Pervak, M. K. Trubetskov, and A. V. Tikhonravov, "Robust synthesis of dispersive mirrors," Opt. Express **19**, 2371–2380 (2011).
16. V. Pervak, V. Fedorov, Y. A. Pervak, and M. Trubetskov, "Empirical study of the group delay dispersion achievable with multilayer mirrors," Opt. Express **21**, 18311–18316 (2013).
17. A. V. Tikhonravov and M. K. Trubetskov, "OptiLayer software," http://www.optilayer.com.
18. C. Skrobol, I. Ahmad, S. Klingebiel, C. Wandt, S. A. Trushin, Z. Major, F. Krausz, and S. Karsch, "Broadband amplification by picosecond OPCPA in DKDP pumped at 515 nm," Opt. Express **20**, 4619–4629 (2012).
19. V. Pervak, A. V. Tikhonravov, M. K. Trubetskov, S. Naumov, F. Krausz, and A. Apolonski, "1.5-octave chirped mirror for pulse compression down to sub-3 fs," Appl. Phys. B **87**, 5–12 (2007).
20. D. Ristau, H. Ehlers, T. Gross, and M. Lappschies, "Optical broadband monitoring of conventional and ion processes," Appl. Opt. **45**, 1495–1501 (2006).
21. T. V. Amotchkina, A. V. Tikhonravov, M. K. Trubetskov, D. Grupe, A. Apolonski, and V. Pervak, "Measurement of group delay of dispersive mirrors with white-light interferometer," Appl. Opt. **48**, 949–956 (2009).
22. M. K. Trubetskov, M. von Pechmann, I. B. Angelov, K. L. Vodopyanov, F. Krausz, and V. Pervak, "Measurements of the group delay and the group delay dispersion with resonance scanning interferometer," Opt. Express **21**, 6658–6669 (2013).
23. V. Pervak, "Recent development and new ideas in the field of dispersive multilayer optics," Appl. Opt. **50**, C55–C61 (2011).
24. A. N. Tikhonov and V. I. Arsenin, *Solutions of Ill-posed Problems* (Winston, 1977).